Ru_2NbGa: A Heusler-type compound with semimetallic characteristics

C. N. Kuo,[1] H. W. Lee,[2] C.-M. Wei,[2] Y. H. Lin,[3] Y. K. Kuo,[3,*] and C. S. Lue[1,†]

[1]*Department of Physics, National Cheng Kung University, Tainan 70101, Taiwan*

[2]*Institute of Atomic and Molecular Sciences, Academia Sinica, Taipei 10617, Taiwan*

[3]*Department of Physics, National Dong Hwa University, Hualien 97401, Taiwan*

(Received 30 August 2016; revised manuscript received 17 October 2016; published 9 November 2016)

The Heusler-type compound of Ru_2NbGa has been successfully synthesized. X-ray analysis confirms that Ru_2NbGa crystallizes in a cubic $L2_1$ structure. The electronic properties of Ru_2NbGa have been characterized by means of the transport and nuclear magnetic resonance (NMR) measurements. The temperature dependence of the electrical resistivity exhibits a typical semimetallic behavior. The NMR spin-lattice relaxation rate shows activated behavior at higher temperatures, attributing to the thermally excited carriers across a pseudogap. We have also deduced a low Fermi-level density of states (DOS), being consistent with the semimetallic characteristic for Ru_2NbGa. In addition, we have performed first-principles total-energy calculations including G_0W_0 and GW_0 corrections for band gaps to investigate the electronic band structure of Ru_2NbGa. The calculated result reveals an indirect overlap between electron and hole pockets that leads to a residual DOS at the Fermi level, providing a consistent explanation for the experimental observations.

DOI: 10.1103/PhysRevB.94.205116

I. INTRODUCTION

Cubic $L2_1$ Heusler compounds (Cu_2MnAl-type) with general formula X_2YZ, where X and Y are two different transition metals and Z often is an element with *sp*-type valence electrons from columns III through VI in the periodic table, have been of considerable interest due to their unusual magnetic and transport properties. Semiconductors, semimetals, normal Pauli metals, weak ferromagnets, antiferromagnets, as well as half-metallic ferromagnets exist in this class of materials [1]. The variety of physical behavior observed in the Heusler series has been related to the strong modifications of the electronic structure near the Fermi level (E_F), as the number of valence electrons per formula unit (Z_t) changes. A theoretical study using the full-potential screened Korringa-Kohn-Rotoker method on the Heusler compounds indicated that the total spin moment per unit cell (M_t) scales with Z_t,following the simple Slater-Pauling rule $M_t = Z_t - 24$ [2]. Accordingly, the net moment disappears with $Z_t = 24$, and the iron-based members such as Fe_2VAl, Fe_2VGa, and Fe_2TiSn have been found to be nonmagnetic [3–9], in agreement with the aforementioned Slater-Pauling relation. Such a relation has also been employed to describe the magnetic properties of other Heusler systems [1,2,10,11]. In addition, many Heusler compounds with $Z_t = 24$ possess narrow band gaps or pseudogaps in the vicinity of E_F. Fe_2VAl which belongs to this prototype has been characterized as a semimetal from intense experimental work [3,12–16]. Its pseudogap features a residual density of states (DOS) along with sharp electronic bands at around E_F which is promising for developing highly efficient thermoelectrics. Indeed, the Fe_2VAl related compounds have been widely studied for improving the thermoelectric figure-of-merit (ZT) through various attempts [17–23].

In this work we add a member of Ru_2NbGa to the list of $Z_t = 24$ Heusler compounds. We have successfully prepared Ru_2NbGa and characterized its electronic properties by means of the transport and ^{93}Nb nuclear magnetic resonance (NMR) measurements. The temperature dependence of the electrical resistivity exhibits semimetallic behavior, viz. a negative temperature coefficient of resistivity together with a finite residual resistivity at low temperatures. The measured Seebeck coefficient is negative, indicating that electrons are dominant carriers responsible for the thermoelectric transport. In addition, the ^{93}Nb NMR spin-lattice relaxation rate shows a combination of Korringa and thermally activated behavior, suggesting that the carriers are thermally excited across a pseudogap between electronic band edges. We have also carried out the electronic structure calculations and the calculated result reveals an indirect overlap between electron and hole pockets that gives rise to a finite Fermi-level density of states. Such a scenario provides a reasonable interpretation for the semimetallic characteristics in Ru_2NbGa established from the present study.

II. EXPERIMENTAL RESULTS AND DISCUSSION

Ru_2NbGa ingots were prepared by an ordinary arc-melting technique. Briefly, the mixture of 99.9% Ru, 99.9% Nb, and 99.999% Ga elemental metals with the stoichiometric ratio was placed in a water-cooled copper hearth and then melted several times in an argon flow arc melter. The weight loss during melting is less than 0.5% for each compound. To promote homogeneity, the as-cast samples were annealed in a vacuum-sealed quartz tube at 800 °C for two days, and then at 400 °C for more than 12 h followed by furnace cooling. This is a typical process to form in a single-phase Heusler compounds [3,17–19,24–26]. A room-temperature x-ray diffraction taken with Cu $K\alpha$ radiation on the powdered specimen is shown in Fig. 1. All diffraction peaks were indexed to the $L2_1$ structure (space group $Fm\bar{3}m$) with a weak impurity peak due to the excess Ru element which has little effect on the present transport and NMR measurements. The unit cell of the Heusler-type Ru_2NbGa based on the $L2_1$ structure is displayed in the inset of Fig. 1. From a further analysis of the x-ray data,

*ykkuo@mail.ndhu.edu.tw

†cslue@mail.ncku.edu.tw

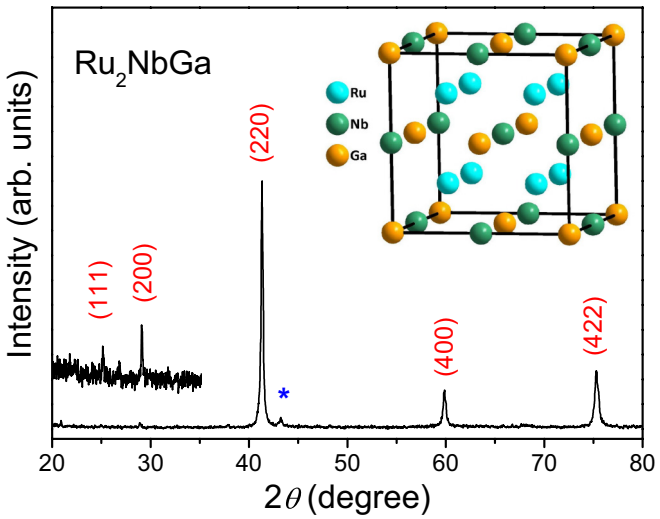

FIG. 1. X-ray diffraction pattern for the powdered Ru_2NbGa. Reflections are indexed with respect to the Cu_2MnAl-type $L2_1$ structure with a weak impurity peak marked by an asterisk. The inset shows the crystal structure of Ru_2NbGa based on the $L2_1$ structure.

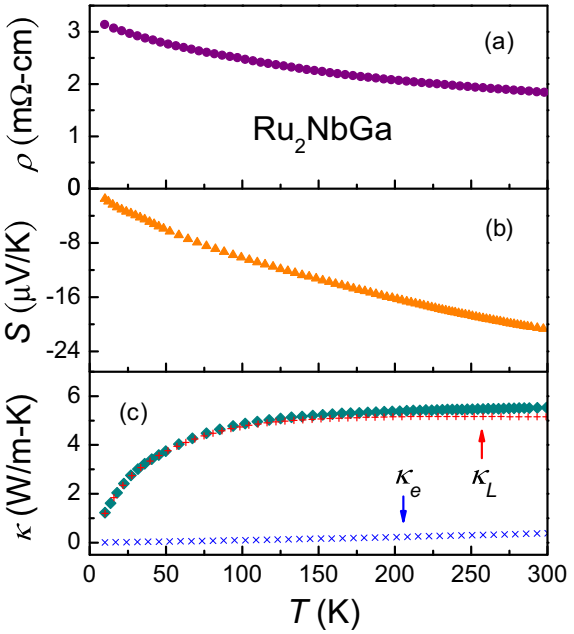

FIG. 2. (a) Electrical resistivity ρ as a function of temperature for Ru_2NbGa. (b) Temperature dependence of the Seebeck coefficient S for Ru_2NbGa. (c) Temperature variations of the total thermal conductivity κ, lattice thermal conductivity κ_L, and electronic thermal conductivity κ_e for Ru_2NbGa.

we determined the lattice constant $a = 6.15$ Å for the Heusler compound of Ru_2NbGa.

It should be noted that the presence of antisite disorder is often found in the Heusler-type compounds with the $L2_1$ structure [1]. While the intensity of (111) peak is quite weak as compared to (220) peak within the $L2_1$ structure, the ratio of diffraction peaks for (111) to (220) is commonly used to judge the degree of the $L2_1$ structural order [27–31]. For the current case of Ru_2NbGa, a relative weak (111) peak has been observed from the enlarged XRD pattern, indicative of the existence of the $L2_1$ structure. However, partial antisite disorder in our sample cannot be ruled out at this stage. In principle, the presence of antisite disorder between Ga and Nb atoms would lead to a diminished (111) peak in Ru_2NbGa. This is likely responsible for the observation of the weakened (111) peak in the XRD pattern.

A. Transport measurements

In Fig. 2(a) we plot the temperature variation of the electrical resistivity $\rho(T)$ for Ru_2NbGa, showing a semiconducting behavior as indicated by its negative temperature coefficient of resistivity. However, this material should be classified as a semimetal due to its finite residual resistivity at low temperatures. Similar $\rho(T)$ features have been found in other semimetallic Heusler compounds such as Fe_2VAl [3,17–19,32]. The activated transport behavior observed in Ru_2NbGa can be realized as the thermally excited carriers across the pseudogap near E_F, in analogy to the case of Fe_2VAl.

The temperature-dependent Seebeck coefficient $S(T)$ of Ru_2NbGa is shown in Fig. 2(b). The measured S is negative in the entire temperature range under investigation. Such a finding suggests that the dominant carriers for the thermoelectric transport are electrons in Ru_2NbGa. The absolute value of S of about 20 μV/K at room temperature is comparable to those potential thermoelectric candidates of Fe_2VAl (~35 μV/K) and Fe_2VGa (~30 μV/K) [17–20,33,34]. It should be noted that many efforts have been made to enhance the magnitude of S in Fe_2VAl by incorporating antisite disorder or by doping at the Al site with various elements [17–21]. As a result, an encouraging enhancement in the absolute value of S up to 130 μV/K has been achieved [17–21]. In this regard, a further improvement in the magnitude of S for Ru_2NbGa via similar attempts would be highly anticipated.

In Fig. 2(c) we display the temperature-dependent thermal conductivity $\kappa(T)$ of Ru_2NbGa. For ordinary metals and semimetals, the total thermal conductivity is a sum of electronic and lattice terms. The electronic thermal conductivity (κ_e) can be evaluated using the Wiedemann-Franz law $\kappa_e \rho / T = L_o$, where ρ is the measured dc electric resistivity and $L_0 = 2.45 \times 10^{-8}$ W Ω K^{-2} is the Lorenz number. The lattice thermal conductivity (κ_L) can be thus obtained by subtracting κ_e from the observed κ. This estimate gives a very small contribution from κ_e, suggesting that the thermal conductivity of Ru_2NbGa is essentially due to κ_L . It is remarkable that the value of κ_L is only 5 W/m K at room temperature which is much smaller than those in Fe_2VAl (~25 W/m K) and Fe_2VGa (~17 W/m K) [18,33,34]. In general, the major difficulty in achieving good thermoelectric performance of materials is to minimize κ_L without deteriorating the power factor ($PF = S^2/\rho$). The common strategy for reducing κ_L of solids can be attained by enhancing the phonon scattering through introducing crystallographic disorder [35,36]. For example, the large κ_L in Fe_2VAl has been effectively reduced to 5 W/m K by substituting tungsten to the vanadium sites [37]. With this respect, the promising low κ_L in Ru_2NbGa has an advantage of improving the $ZT = S^2T/\rho\kappa$ for thermoelectric applications.

The inherent low κ_L in Ru_2NbGa is very likely related to structural disorder which is evidenced by the lack of the peak feature at low temperatures. In general, the height of the low-T peak in κ_L reflects the degree of structural order since crystallographic disorder has an effect to suppress the low-T peak. As a matter of fact, the disappearance of the peak feature in κ_L driven by disorder has been reported in the Heusler-type $Fe_2VAl_{1-x}Si_x$ compounds [25,26].

B. NMR measurements

Nuclear magnetic resonance is known as a local probe yielding information about Fermi surface features. In this study, we have carried out the ^{93}Nb NMR measurements on powdered Ru_2NbGa specimens under a constant field of 7.08 T. Central transition line shapes were obtained from spin echo fast Fourier transforms using a standard $\pi/2$-τ-π sequence. Several representative spectra taken at various temperatures are given in the inset of Fig. 3. As one can see, the spectrum shows slight broadening upon cooling while the corresponding Knight shift ^{93}K remains almost unchanged. Here ^{93}K is determined from the position of the maximum of each spectrum with respect to an aqueous $KNbCl_6$. We found that the magnitude of $^{93}K = 0.46\%$ is quite large for a semimetallic material with a small residual DOS at E_F. Therefore, the conduction electrons at the Fermi surfaces should have a minor contribution to ^{93}K . Rather, the observed ^{93}K mainly arises from the orbital electrons which generate the orbital shift [38]. Similar mechanisms employed for the realization of large Knight shifts in other semimetallic Heusler systems such as Fe_2VAl and Fe_2VGa have been reported [12,39].

The ^{93}Nb NMR spin-lattice relaxation rate was obtained by integrating the spin echo signal using the inversion recovery method. The temperature variation of ^{93}Nb $1/T_1$ of Ru_2NbGa is illustrated in Fig. 3, showing a linear increase upon heating

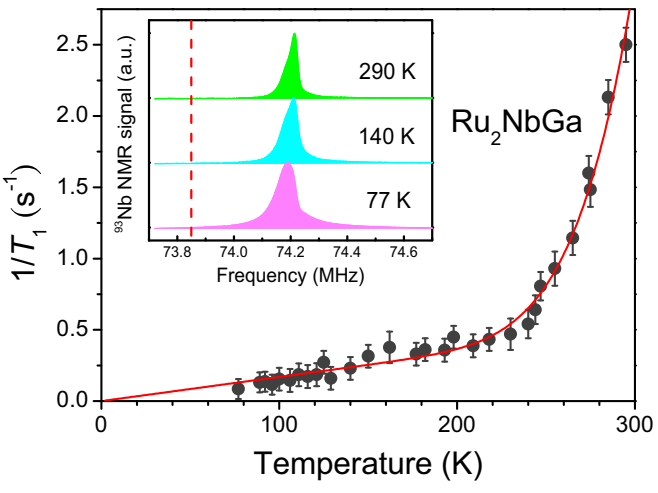

FIG. 3. Temperature dependence of the ^{93}Nb spin-lattice relaxation rate for Ru_2NbGa. Solid curve: Fit to the Korringa plus activated behavior described in the text. Inset: Representative ^{93}Nb NMR central transition spectra of Ru_2NbGa measured at various temperatures. The dashed vertical line denotes the position of the ^{93}Nb reference frequency.

and then a rapid rise above 220 K. Similar features have been found in ^{51}V $1/T_1$ of Fe_2VAl and Fe_2VGa [12,13,39], ^{27}Al $1/T_1$ of $RuAl_2$ and $CaAl_2Si_2$ [40,41], as well as ^{59}Co $1/T_1$ of $(La, Ca)_xCo_4Sb_{12}$ and CoTiSb [42–44]. Those observations have been well described by the Korringa process together with an additional contribution from activated behavior. In analogy to those cases, we fit ^{93}Nb $1/T_1$ of Ru_2NbGa to the expression $AT + BT^2 \exp(-E_a/2k_BT)$, where A, B, and E_a are fitting parameters. The first term here is characterized by the Korringa relation (constant $1/T_1T$) which is due to the relaxation of the conduction electrons [45]. The second term arises from the additional contribution via thermally excited carriers across an activation energy E_a. The band dispersion here was approximated by the square root of the energy near each band edge. The corresponding carrier density of the conduction electrons varies with temperature according to $T^{3/2}\exp(-E_a/2k_BT)$. The optimum fit with $A = 1.7 \pm 0.3 \times 10^{-3}$ s^{-1} K^{-1}, $B = 4.6 \pm 0.4 \times 10^{-2}$ s^{-1} K^{-2}, and $E_a = 0.38 \pm 0.03$ eV is shown as a solid curve over the entire temperature range in Fig. 3. It is remarkable that the extracted E_a of about 0.38 eV is quite close to the magnitude of the pseudogap obtained from theoretical electronic structure calculations which will be described in the following section. With this respect, we have a concise picture that the activated behavior in ^{93}Nb $1/T_1$ could be attributed to the thermally excited carriers across the pseudogap in Ru_2NbGa.

The Korringa process for the relaxation of Nb nuclear spins in Ru_2NbGa is dominated by the Nb 4d electrons and can be expressed as [45]

$$\frac{1}{T_1T} = 2hk_B\left[{}^{93}\gamma_n H_{\rm hf}^d N_d(E_F)\right]^2. \quad (1)$$

Here $^{93}\gamma_{\rm n}$ is the Nb nuclear gyromagnetic ratio, $H_{\rm hf}^d$ is the hyperfine field per spin of the Nb d electrons, and $N_d(E_F)$ is the Nb 4d Fermi-level DOS in units of states/eV spin. Taking $H_{\rm hf}^d \sim -2.1 \times 10^5$ G for Nb metal [46,47], the experimental value of $A = 1.7 \times 10^{-3}$ s^{-1} K^{-1} would yield $N_d(E_F) = 0.07$ states/eV fu. Note that this value is an order of magnitude smaller than those in Nb-based metals [46–48], supporting the scenario of the semimetallic nature for Ru_2NbGa.

C. Electronic structure calculations

In order to substantiate our experimental perspectives and gain a further insight on the electronic structure of Ru_2NbGa, we have performed the first-principles total-energy calculations including G_0W_0 and GW_0 [49] for the band gaps using PBE [50] and HSE06 [51] initial wave functions. All first-principles calculations are implemented in Vienna *ab initio* simulation package (VASP) [52] and the band structures are obtained from Wannier-interpolation band scheme using Wannier90 code [53,54]. K-point sampling for all calculations is Γ-centered Monkhorst-Pack [55] $12 \times 12 \times 12$. The kinetic energy cutoff is 410 eV and the lattice constant is kept at the experimental value. For the G_0W_0 and GW_0 calculations, total bands are 168, including 138 empty states.

As shown in Fig. 4, the band structures of Ru_2NbGa indicate that it is a semimetal with a negative band gap (so-called pseudogap) of -0.53 eV and narrow-band semiconductor with a band gap of 0.07 eV, using PBE and HSE06 functionals,

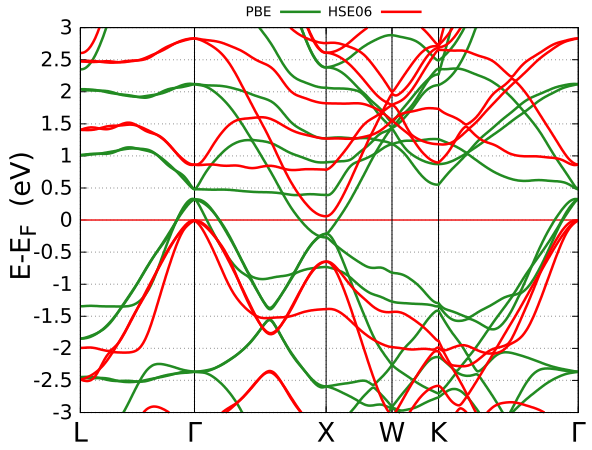

FIG. 4. Band structures obtained from PBE and HSE06 functionals. The zero of energy is placed at the Fermi level.

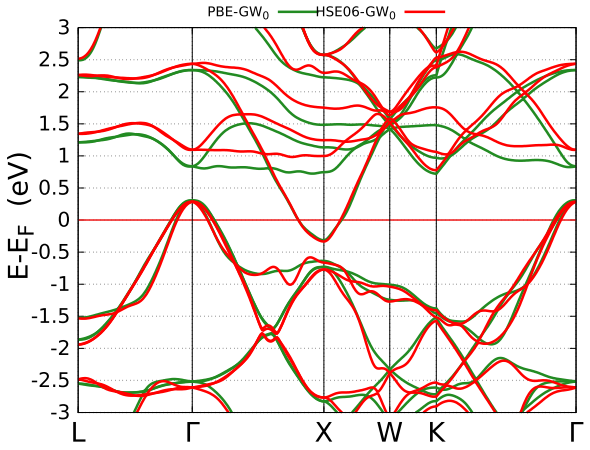

FIG. 6. GW_0 band structures using PBE and HSE06 initial wave functions for Ru_2NbGa.

respectively. The results of these two functionals are somewhat controversial and such phenomena have been also reported in the prototype of Fe_2VAl [56–59]. As mentioned above, the DFT results obtained strongly depend on the exchange correlation functional used and thus a correct procedure to resolve this discrepancy is highly desirable. It is well known that many-body GW approximation could render a better estimation of a band gap, we thus have also included many-body G_0W_0 and GW_0 corrections to the calculations.

The G_0W_0 and GW_0 calculated band structures of ordered $L2_1$ Ru_2NbGa are shown in Figs. 5 and 6, respectively. The results reveal that either PBE or HSE06 initial functions Ru_2NbGa exhibits a semimetallic character in both G_0W_0 and GW_0 calculations. Moreover, these band gaps are very close in values as listed in Table I and the largest difference is only 0.14 eV. Furthermore, we also have applied the same procedure to Fe_2VAl, and obtained a similar tendency where G_0W_0 and GW_0 calculated band structures have consistent features with different exchange correlation functionals used. Consequently, it appears that correct band-gap structures of such materials can be obtained by exploiting G_0W_0 and GW_0 many-body corrections.

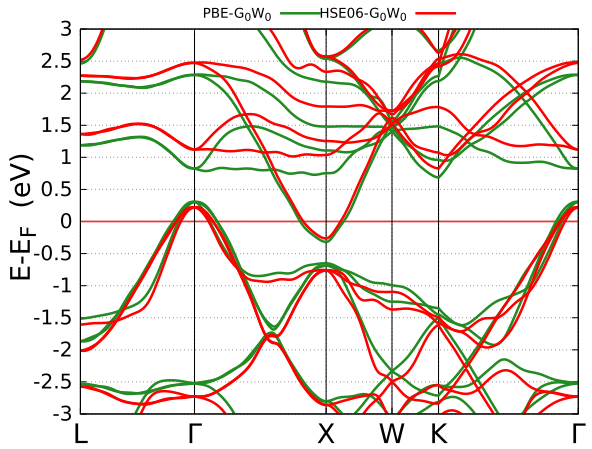

FIG. 5. G_0W_0 band structures using PBE and HSE06 initial wave functions for Ru_2NbGa.

In the vicinity of E_F, there are three hole degenerate pockets at the Γ point, compensated by one electron pocket centered at the X point. The hole pockets at Γ are dominated by the Ru 4d t_{2g} bands with a small admixture of Nb t_{2g} orbitals while the electron pocket at the X is purely Nb 4d e_g orbitals. An overlap between hole and electron pockets crossing E_F gives rise to a semimetallic character for Ru_2NbGa. It is remarkable that the magnitude of the pseudogap is in satisfactory agreement with the value of 0.38 eV deduced from the ^{93}Nb NMR $1/T_1$. On this basis, the activated behavior of $1/T_1$ at high temperatures could be reasonably realized as the thermal excitation of carriers across the pseudogap.

Figure 7 illustrates the calculated HSE06-G_0W_0 total and site-decomposed DOS of Ru_2NbGa as a representative. It is apparent that the total DOS spectrum consists of two peaks which are separated by a steep hybridization pseudogap centered at E_F with residual Fermi-level DOS of 0.16–0.22 states/eV fu. We also determined the Nb partial 4d DOS of 0.06–0.08 states/eV fu at E_F. Remarkably, this value is quite consistent with 0.07 states/eV fu obtained from the analysis of the Korringa relation. With these accordances, it reinforces the conclusion that the G_0W_0 and GW_0 calculations using two different initial wave functions give consistent results with good agreement with experimental observations. We thus conclude here that the inclusion of the many-body G_0W_0 and/or GW_0 effects is crucial to obtain correct band structures of the full Heusler compounds.

TABLE I. The calculated band gap in unit of eV, total DOS at the Fermi level [$N(E_F)$], and the Nb partial 4d Fermi-level DOS [$N_d(E_F)$] in units of states/eV fu.

Method	Gap	$N(E_F)$	$N_d(E_F)$
PBE	−0.53	0.22	0.08
G_0W_0@PBE	−0.62	0.20	0.05
GW_0@PBE	−0.62	0.19	0.05
HSE	0.07	0.00	0.00
G_0W_0@HSE	−0.48	0.16	0.06
GW_0@HSE	−0.62	0.20	0.08

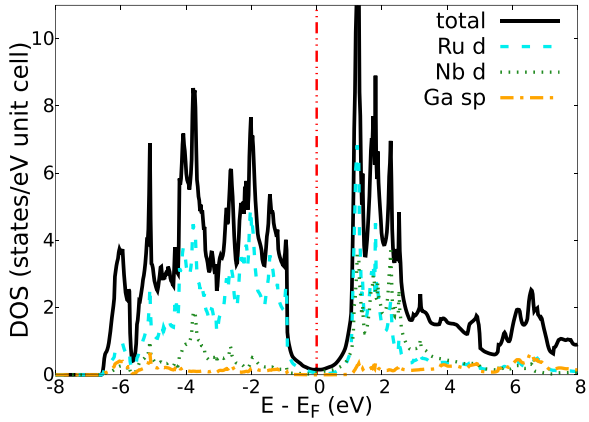

FIG. 7. The HSE06-G_0W_0 total and site-decomposed density of states of Ru_2NbGa. The Fermi level is set at zero.

III. CONCLUSIONS

We have successfully synthesized a Heusler-type compound Ru_2NbGa and characterized its electronic properties by means of the transport and NMR measurements. The semimetallic nature in Ru_2NbGa has been clearly evidenced by the observations of the thermally activated behavior, pointing out the existence of a pseudogap at around the Fermi level. First-principles total-energy calculations including G_0W_0 and GW_0 band corrections further indicate that the pseudogap arises from an indirect overlap between the electron and hole pockets, leading to a small Fermi-level DOS as observed. We highlighted that the thermoelectric features of Ru_2NbGa behave in a similar manner to those observed in the semimetallic Heusler compounds, suggesting that Ru_2NbGa has an inherent potential for possible thermoelectric applications.

ACKNOWLEDGMENTS

This work was supported by the Ministry of Science and Technology of Taiwan under Grants No. MOST-103-2112-M-006-014-MY3 (C.S.L.), No. MOST-103-2112-M-259-008-MY3 (Y.K.K.), and No. MOST-105-2923-M-006-002-MY3 (C.S.L.). H.W.L. thanks Dr. Cheng-Rong Hsing for valuable discussions about GW calculations.

[1] T. Graf, C. Felser, and S. S. P. Parkin, Prog. Solid State Chem. **39**, 1 (2011), and references therein.
[2] I. Galanakis, P. H. Dederichs, and N. Papanikolaou, Phys. Rev. B **66**, 174429 (2002).
[3] Y. Nishino, M. Kato, S. Asano, K. Soda, M. Hayasaki, and U. Mizutani, Phys. Rev. Lett. **79**, 1909 (1997).
[4] C. S. Lue, J. H. Ross, Jr., C. F. Chang, H. D. Yang, Phys. Rev. B **60**, R13941 (1999).
[5] C. S. Lue, Y. Li, J. H. Ross, Jr., and G. M. Irwin, Phys. Rev. B **67**, 224425 (2003).
[6] A. Slebarski and J. Goraus, Phys. Rev. B **80**, 235121 (2009).
[7] C. S. Lue, J. H. Ross, Jr., K. D. D. Rathnayaka, D. G. Naugle, S. Y. Wu, and W.-H. Li, J. Phys.: Condens. Matter **13**, 1585 (2001).
[8] A. Slebarski, M. B. Maple, E. J. Freeman, C. Sirvent, D. Tworuszka, M. Orzechowska, A. Wrona, A. Jezierski, S. Chiuzbaian, and M. Neumann, Phys. Rev. B **62**, 3296 (2000).
[9] A. Slebarski, J. Deniszczyk, W. Borgiel, A. Jezierski, M. Swatek, A. Winiarska, M. B. Maple, and W. M. Yuhasz, Phys. Rev. B **69**, 155118 (2004).
[10] I. Galanakis, J. Phys.: Condens. Matter **16**, 3089 (2004).
[11] S. Skaftouros, K. Ozdogan, E. Sasioglu, and I. Galanakis, Phys. Rev. B **87**, 024420 (2013).
[12] C. S. Lue and J. H. Ross, Jr., Phys. Rev. B **58**, 9763 (1998).
[13] C. S. Lue and J. H. Ross, Jr., Phys. Rev. B **61**, 9863 (2000).
[14] H. Okamura, J. Kawahara, T. Nanba, S. Kimura, K. Soda, U. Mizutani, Y. Nishino, M. Kato, I. Shimoyama, H. Miura, K. Fukui, K. Nakagawa, H. Nakagawa, and T. Kinoshita, Phys. Rev. Lett. **84**, 3674 (2000).
[15] Y. Nishino, H. Sumi, and U. Mizutani, Phys. Rev. B **71**, 094425 (2005).
[16] C. S. Lue, R. F. Liu, M. Y. Song, K. K. Wu, and Y. K. Kuo, Phys. Rev. B **78**, 165117 (2008).
[17] Y. Nishino, H. Kato, M. Kato, and U. Mizutani, Phys. Rev. B **63**, 233303 (2001).
[18] C. S. Lue and Y.-K. Kuo, Phys. Rev. B **66**, 085121 (2002).
[19] M. Vasundhara, V. Srinivas, and V. V. Rao, J. Phys.: Condens. Matter **17**, 6025 (2005).
[20] Y. Nishino, S. Deguchi, and U. Mizutani, Phys. Rev. B **74**, 115115 (2006).
[21] M. Vasundhara, V. Srinivas, and V. V. Rao, Phys. Rev. B **77**, 224415 (2008).
[22] D. I. Bilc, G. Hautier, D. Waroquiers, G.-M. Rignanese, and P. Ghosez, Phys. Rev. Lett. **114**, 136601 (2015).
[23] H. Al-Yamani and B. Hamad, J. Electron. Mater. **45**, 1101 (2016).
[24] C. S. Lue and Y. K. Kuo, J. Appl. Phys. **96**, 2681 (2004).
[25] C. S. Lue, Y.-K. Kuo, S.-N. Horng, S. Y. Peng, and C. Cheng, Phys. Rev. B **71**, 064202 (2005).
[26] C. S. Lue, C. F. Chen, J. Y. Lin, Y. T. Yu, and Y.-K. Kuo, Phys. Rev. B **75**, 064204 (2007).
[27] E. Popiel, M. Tuszynski, W. Zarek, and T. Rendecki, J. Less-Common Met. **146**, 127 (1989).
[28] Y. Feng, J. Y. Rhee, T. A. Wiener, D. W. Lynch, B. E. Hubbard, A. J. Sievers, D. L. Schlagel, T. A. Lograsso, and L. L. Miller, Phys. Rev. B **63**, 165109 (2001).
[29] I. Maksimov, D. Baabe, H. H. Klauss, F. J. Litterst, R. Feyerherm, D. M. Tobbens, and A. Matsushita, and S. Sullow, J. Phys.: Condens. Matter **13**, 5487 (2001).
[30] M. Yin and P. Nash, J. Alloys Compd. **634**, 70 (2015).
[31] N. Naghibolashrafi, S. Keshavarz, V. I. Hegde, A. Gupta, W. H. Butler, J. Romero, K. Munira, P. LeClair, D. Mazumdar, J. Ma, A. W. Ghosh, and C. Wolverton, Phys. Rev. B **93**, 104424 (2016).
[32] A. Matsushita, T. Naka, Y. Takano, T. Takeuchi, T. Shishido, and Y. Yamada, Phys. Rev. B **65**, 075204 (2002).

[33] C. S. Lue, W. J. Lai, C. C. Chen, and Y.-K. Kuo, J. Phys.: Condens. Matter **16**, 4283 (2004).
[34] C. S. Lue, J. W. Huang, D. S. Tsai, K. M. Sivakumar, and Y.-K. Kuo, J. Phys.: Condens. Matter **20**, 255233 (2008).
[35] C. S. Lue, M. D. Chou, N. Kaurav, Y. T. Chung, and Y. K. Kuo, Appl. Phys. Lett. **94**, 192105 (2009).
[36] C. S. Lue, Y. S. Tseng, J. Y. Huang, H. L. Hsieh, H. Y. Liao, and Y. K. Kuo, AIP Adv. **3**, 072132 (2013).
[37] M. Mikami, Y. Kinemuchi, K. Ozaki, Y. Terazawa, and T. Takeuchi, J. Appl. Phys. **111**, 093710 (2012).
[38] Edited by G. C. Carter, L. H. Bennett, and D. J. Kahan, *Metallic Shifts in NMR* (Pergamon, Oxford, 1977).
[39] C. S. Lue and J. H. Ross, Jr., Phys. Rev. B **63**, 054420 (2001).
[40] E. A. Hill, P. Volkov, S. J. Poon, and Y. Wu, Phys. Rev. B **51**, 4865 (1995).
[41] C. S. Lue, S. Y. Wang, and C. P. Fang, Phys. Rev. B **75**, 235111 (2007).
[42] C. S. Lue, S. M. Huang, C. N. Kuo, F.-T. Huang, and M.-W. Chu, New J. Phys. **10**, 083029 (2008).
[43] C. S. Lue and S. C. Chen, Phys. Rev. B **79**, 125108 (2009).
[44] C. S. Lue, C. F. Chen, F.-K. Chiang, and M.-W. Chu, Phys. Rev. B **80**, 174202 (2009).
[45] J. Korringa, Physica **16**, 601 (1950).
[46] C. S. Lue, T. H. Su, B. X. Xie, and C. Cheng, Phys. Rev. B **74**, 094101 (2006).
[47] T. H. Su, C. S. Lue, and Y. K. Kuo, J. Appl. Phys. **104**, 093709 (2008).
[48] C. S. Lue, T. H. Su, H. F. Liu, and B.-L. Young, Phys. Rev. B **84**, 052509 (2011).
[49] M. Shishkin and G. Kresse, Phys. Rev. B **75**, 235102 (2007).
[50] J. P. Perdew, K. Burke, and M. Ernzerhof, Phys. Rev. Lett. **77**, 3865 (1996).
[51] A. V. Krukau, O. A. Vydrov, A. F. Izmaylov, and G. E. Scuseria, J. Chem. Phys. **125**, 224106 (2006).
[52] G. Kresse and J. Furthmuller, Phys. Rev. B **54**, 11169 (1996).
[53] A. A. Mostofi, J. R. Yates, Y.-S. Lee, I. Souza, D. Vanderbilt, and N. Marzari, Comput. Phys. Commun. **178**, 685 (2008).
[54] D. R. Hamann and D. Vanderbilt, Phys. Rev. B **79**, 045109 (2009).
[55] H. J. Monkhorst and J. D. Pack, Phys. Rev. B **13**, 5188 (1976).
[56] G. Y. Guo, G. A. Botton, and Y. Nishino, J. Phys.: Condens. Matter **10**, L119 (1998).
[57] D. J. Singh and I. I. Mazin, Phys. Rev. B **57**, 14 (1998).
[58] D. I. Bilc and P. Ghosez, Phys. Rev. B **83**, 205204 (2011).
[59] D. Do, M.-S. Lee, and S. D. Mahanti, Phys. Rev. B **84**, 125104 (2011).